The Astrophysical Journal, 678:1471–1479, 2008 May 10

ION ANISOTROPY AND HIGH-ENERGY VARIABILITY OF LARGE SOLAR PARTICLE EVENTS: A COMPARATIVE STUDY

Lun C. Tan,[1] Donald V. Reames, and Chee K. Ng[2]
NASA Goddard Space Flight Center, Greenbelt, MD 20771
Received 2007 September 12; accepted 2008 January 9

ABSTRACT

We have made comparative studies of ion anisotropy and high-energy variability of solar energetic particle (SEP) events previously examined by the Solar, Heliospheric, and Interplanetary Environment (SHINE) Workshop campaign. We have found distinctly different characteristics of SEPs in two large "gradual" events having very similar solar progenitors (the 2002 April 21 and August 24 events). Since the scattering centers of SEPs are approximately frozen in the solar wind, we emphasize work in the solar-wind frame, where SEPs tend to be isotropized and small anisotropies are easier to detect. While in the August event no streaming reversal occurred, in the April event the field-aligned anisotropy of all heavy ions showed signs of streaming reversal. The difference in streaming reversal was consistent with the difference in the presence of the outer reflecting boundary. In the April event the magnetic mirror, which was located behind the interplanetary shock driven by the preceding coronal mass ejection (CME), could block the stream of SEPs, while in the August event SEPs escaped freely in the absence of any nearby boundary. The magnetic mirror was formed at the bottleneck of magnetic field lines draped around a flank of the preceding CME. In previous SHINE event analysis, the contrasting event durations and Fe/O ratios of the both events were explained as the interplay between shock geometry and seed population. Our new findings, however, indicate that event duration and time, as well as spectral variation, are also affected by the presence of a nearby reflecting boundary.

Subject headings: acceleration of particles — interplanetary medium — shock waves — Sun: coronal mass ejections (CMEs) — Sun: particle emission

1. INTRODUCTION

1.1. *Significance of Investigating High-Energy Variability of SEP Events*

One issue of concern to the National Space Weather Program[3] is the investigation of high-energy variability of spectral and composition characteristics of gradual SEP events. We seek to discover the origin of that variability, and how it relates to outstanding questions in solar-terrestrial physics.

Examination of particle spectral and composition characteristics in various SEP events is widely used to investigate the injection, acceleration, and transport of SEPs (see Reames 1999). Observed spectral characteristics, however, strongly depend on the longitude of the point at which the observer's magnetic flux tube connects to the CME-driven shock (e.g., Reames et al. 1996). There exists an east-west asymmetry of intensity-time profiles of SEPs; western SEP events reach peak intensities earlier than eastern events (e.g., Cane et al. 1988) because of the Archimedean spiral structure of the interplanetary magnetic field (IMF). In order to diminish the influence of solar longitude effects, it is preferable to make comparative studies of SEP events that have very similar solar progenitors.

Often, two gradual SEP events having very similar solar progenitors show similar characteristics at ion energies less than $\sim$10 MeV nucleon^{-1}, but at higher energies may exhibit extreme differences in their characteristics, including abundance ratios, event size, spectral shape, GeV ion content, and event duration (Tylka et al. 2005). Carrying out comparative studies on these differences can improve our understanding of the generation and propagation of SEPs, and be of benefit in forecasting the space radiation environment.

1.2. *The Solar, Heliospheric, and Interplanetary Environment (SHINE) Workshop Campaign*

The SHINE workshop[4] encouraged a concerted, focused effort to investigate a few carefully selected "campaign" SEP events. Two famous examples of SHINE events are the 2002 April 21 and August 24 events examined in Tylka et al. (2005, 2006), and Tylka & Lee (2006). The April and August events had their flare locations at S14°, W84° and S02°, W81°, and CME speeds of 2400 and 1900 km s^{-1}, respectively. In both events, the size of the associated flares was nearly same. The solar wind speed and the transit time of interplanetary (IP) shocks were also comparable. In addition, both events were accompanied by metric and DH type III and type II radio emissions (Tylka et al. 2006).

At ion energies between $\sim$0.5 and $\sim$10 MeV nucleon^{-1}, the two events had nearly the same event-averaged Fe/O ratio. At higher energies, however, the ratio differed by nearly 2 orders of magnitude; in the April event the ratio fell to only $\sim$10% of the nominal coronal value, but in the August event the ratio rose to $\sim$6 times the coronal value (see Tylka et al. 2006, their Fig. 1). In addition, at $\sim$10 MeV the proton intensity-time profile in both events showed similar evolution patterns, but at higher energies the duration of proton intensities was distinctly different (see Fig. 11 of Tylka et al. 2005). The full width half-maximum (FWHM) of proton intensities at >100 in the April event was $\sim$20 hr, in contrast to $\sim$2 hr in the August event.

Tylka et al. (2005, 2006) and Tylka & Lee (2006) attributed the difference between the two events to the interplay between two factors involved in the ion acceleration by CME-driven

[1] Also at: Perot Systems, Fairfax, VA 22031; ltan@mail630.gsfc.nasa.gov.
[2] Also at: Department of Astronomy, University of Maryland, College Park, MD 20742.
[3] See http://www.nsf.gov/pubs/2007/nsf07010/nsf07010.jsp.
[4] See http://cdaw.gsfc.nasa.gov/SHINE_Campaign/index.html.

shocks (see Fig. 2 of Tylka et al. 2005): the evolution in the geometry of CME-driven shocks, which generally begins as quasi-perpendicular near the Sun but evolves toward quasi-parallel as the shock moves outward; and a compound seed population, typically consisting of suprathermals from the corona or solar wind and from small impulsive flares. The quasi-parallel shock (Lee 1983) remains in contact with a given group of magnetic flux tubes for an extended period and has small injection energy requirement, resulting in a long duration of accelerated particle events and a seed population similar to solar wind suprathermals. In contrast, the quasi-perpendicular shock has a short contact period and a high injection energy requirement, preferentially accelerating seed particles from flares within a short period.

1.3. *Importance of Anisotropy Analysis of SEPs*

So far, the high-energy variability of SEP events has been examined mainly by using ion composition or energy spectral data. In addition to the ion composition or energy spectral measurement, however, the ion anisotropy analysis is an independent way to examine the high-energy variability of SEP events. In fact, SEP angular distributions are more direct means to study particle transportation in the interplanetary medium (Reames & Ng 2002).

Recently, Tan et al. (2007) carried out an anisotropy analysis of gradual SEP events in the 2–8 MeV nucleon^{-1} range by using the Low-Energy Matrix Telescope (LEMT) data from the *Wind* spacecraft (von Rosenvinge et al. 1995). So far, the *Wind*/LEMT sensor has provided the best resolution of ion angular distributions in the MeV nucleon^{-1} range (see Reames et al. 2001). The analysis began by introducing the concept of the "rest" frame, in which the phase-space distribution function of ions is assumed to be isotropic (Gloeckler et al. 1984). The velocity of the rest frame relative to the spacecraft frame is the ion bulk flow velocity $\boldsymbol{V}_F$, which can be calculated from ion-sectored count rate data at a given ion energy. Since in the solar wind frames the first-order anisotropy vectors $\boldsymbol{A}_{1s}$ can be easily deduced from $\boldsymbol{V}_F$ (Forman 1970; Tan et al. 1992a), we started from the $\boldsymbol{V}_F$ analysis in order to examine anisotropic characteristics of SEPs. In two large events (the 1998 September 30 and 2001 September 24 events) among three SEP events examined in Tan et al. (2007), the flow reversal of heavy ions was observed in the spacecraft frame, while protons kept their flow direction continuously.

One potential explanation as to why only heavy ions reverse their flow direction is that, in the given MeV nucleon^{-1} range, softening spectra at the local IP shock may provide mainly accelerated protons, but fewer heavy ions (see Desai et al. 2003, 2004; Tylka et al. 2005, 2006). Consequently, heavy ions predominantly come from early acceleration near the Sun, and propagate across 1 AU. Beyond 1 AU, there is evidence (Bieber et al. 2002; Reames & Ng 2002; Tan et al. 2007) indicating the possible existence of a nearby reflecting boundary of SEPs, due to the transient structure of IMF driven by preceding CMEs. In fact, downstream of the IP shock a magnetic mirror can be formed in the bottleneck of magnetic field lines draped around a flank of preceding CME (Tan et al. 1992b; Bieber et al. 2002). The magnetic bottleneck plays the role of an outer reflecting boundary for the SEPs. Forward-streaming particles encountering the boundary could be reflected back to 1 AU to enhance the backward stream of particles.

1.4. *IMF Configuration in the 2001 September 24 Event*

Since the presence of transient reflecting boundary of SEPs should be traceable from the observations of IMF and solar wind, we will reanalyze these observations in the 2001 September 24 event previously examined in Tan et al. (2007) over a longer period prior to the occurrence of the primary CME 2. The time profiles of the strength B of IMF and the speed V_{sw} of solar wind from *Wind* observations are plotted in the top panel of Figure 1, starting from $\sim$1 week prior to the occurrence of CME 2. The largest jump in both B and V_{sw} occurred at time t_{obs}(Shock 2), indicating the arrival of the IP shock (Shock 2) prior to the primary CME 2, whose launch time was September 24 10:16 (UT) (linear fitting),[5] as denoted by t_{laun}(CME 2) in Figure 1.

Before the primary CME 2, there was also a preceding CME 1. The *Wind* spacecraft observed the IP shock prior to CME 1 at t_{obs}(Shock 1) = September 23 09:18 (UT), prior to the launch of CME 2. The observed solar wind speed after t_{obs}(Shock 1) was $V_{sw1} \sim 600$ km s^{-1}. Assuming that the average CME speed between the Sun and 1 AU was between V_{sw1} and $3V_{sw1}$, the launch time t_{laun}(CME 1) of the preceding CME 1 should be between September 20 12:00 (UT) and September 22 10:00 (UT). During this time interval there were 16 CME events observed. Fortunately, only one CME event had a linear speed greater than 500 km s^{-1}. That CME event, with a linear speed of 659 km s^{-1}, should be identified as CME 1, whose launch time t_{laun}(CME 1) was September 21 08:48 (UT) (linear fitting).

Since the magnetic bottleneck can be formed by the magnetic field lines draped around a flank of the preceding CME (Tan et al. 1992b; Bieber et al. 2002), the morphology of field lines behind Shock 1 should be essential to particle transport. We hence show the field of view (FOV) for the preceding CME 1 as observed by the Large Angle and Spectrometric Coronagraph (LASCO)/C2 telescope on board of the *SOHO* spacecraft at September 21 10:54 (UT) in the middle left panel of Figure 1; CME 1 is in the southeast quadrant, with its central position angle (CPA) of 135°.

Furthermore, the event-associated flare was located at S19°, E63°. Assuming an axial symmetric expansion of the preceding CME 1, in the middle right panel of Figure 1 we schematically draw the envelop of the CME material in the solar wind (the "interplanetary coronal mass ejection (ICME)"; see Cane & Richardson 2003) as projected on the ecliptic plane at $t = t_{laun}$(CME 2), at that time the primary CME 2 was still near the Sun, while the radial separation Δr between the leading edge of CME 1 and the *Wind* spacecraft was small ($\sim$0.34 AU). From the cartoon in Figure 1, one can see that the *Wind* spacecraft was located on "open" field lines. Because of the high speed of CME 1, however, the field lines draped around the western flank of CME 1 would be compressed in the region between Shock 1 and CME 1, leading to the formation of a magnetic bottleneck, which plays the role of a reflecting boundary for SEPs.

1.5. *Effect of Nearby Reflecting Boundary on Particle Transport*

An intuitive speculation is that in analogy to building a dam in a stream, when the water level and storage time in the reservoir increase, the reflecting boundary that blocks the flux tube would increase the peak intensity and duration of high-energy particles inside the tube, leading to a larger particle fluence, which is the particle intensity integrated over the SEP event period. It is noticeable that observational evidence indeed supports this speculation. For example, Roelof et al. (1992) noted that an inner heliospheric "reservoir" of SEPs could be formed behind a magnetic structure that is created earlier by a superposition of plasma disturbances that inhibit the escape of SEPs. Sarris & Malandraki (2003) found that the electron event occurring within a converging IMF structure exhibits a remarkably longer decay

[5] See http://cdaw.gsfc.nasa.gov/CME_list.

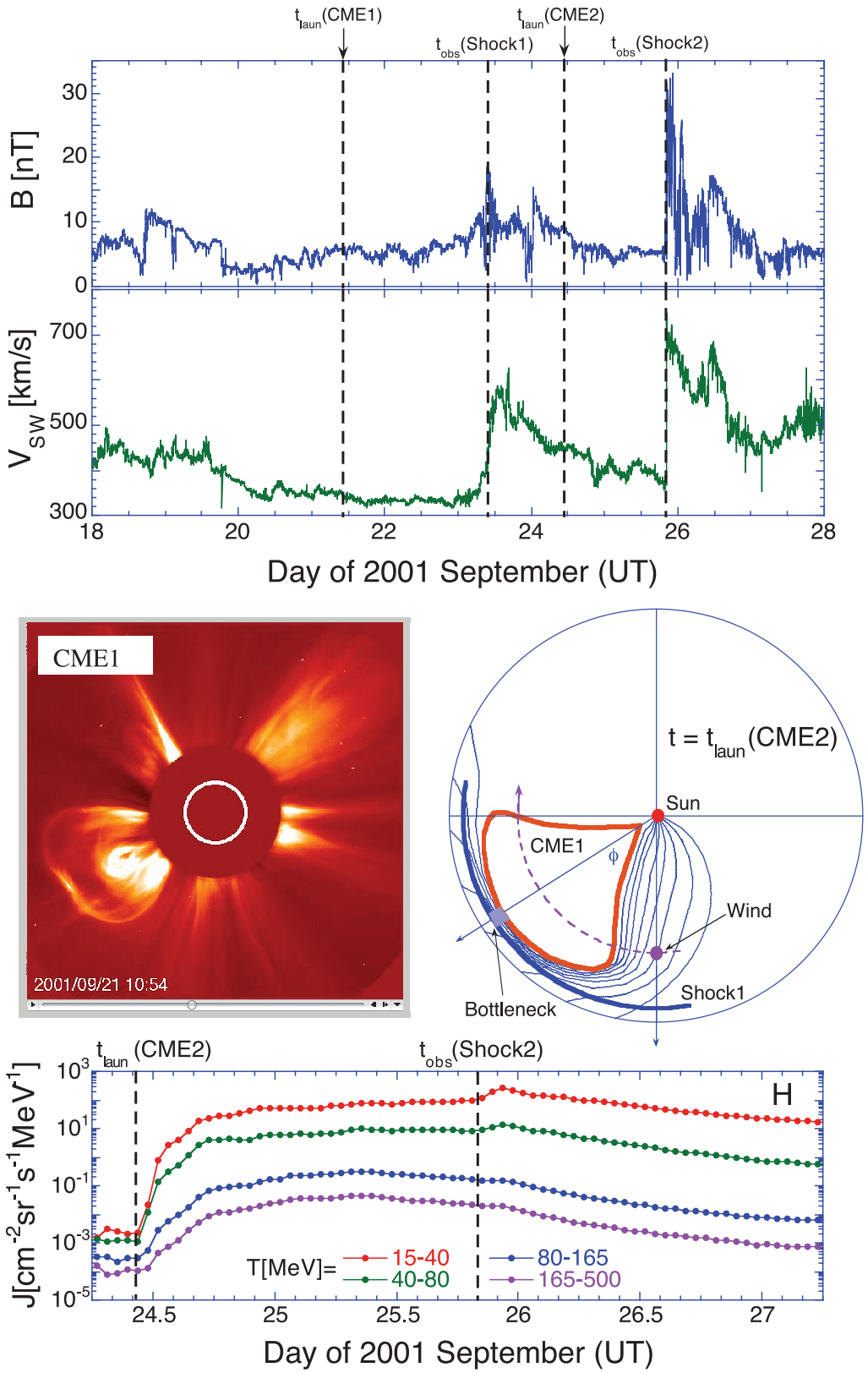

FIG. 1.—*Top*: Time profiles of the strength B of IMF and the speed V_{sw} of solar wind in the 2001 September 24 event, where t_{laun} and t_{obs} are the launch time of CMEs and the observation time of IP shocks, respectively. *Middle*: Field of view for the preceding CME 1 as measured by the LASCO/C2 telescope (*left*) and the IMF configuration in the 2001 September 24 event (*right*; see text). *Bottom*: Intensity-time profiles of high-energy protons as deduced from *GOES-8* data in the 2001 September 24 event.

phase than an event occurring within a diverging IMF structure. In addition, Reames et al. (1996) and Ng et al. (2003) calculated the decay time of ions trapped behind the shock and found that it is independent of ion energies. Also, Kocharov et al. (2005) simulated the intensity of high-energy protons in a closed loop of IMF and found that inside the loop there is a nearly perfect exponential decay of proton intensities, with the decay time being significantly longer than that predicted by the usual diffusion-convection model.

Our speculation is also supported by observation of the 2001 September 24 event. Since the flow reversal of heavy ions (Tan et al. 2007) and the presence of the preceding CME (top panels in Fig. 1) are observable, according to our speculation the September event should have a high peak intensity and long duration of high-energy protons. As shown in the bottom panel of Figure 1, the *GOES-8* proton data confirm this speculation.

1.6. *Questions to be Addressed in This Work*

We wish to add the anisotropy analysis of SEPs to the examination of both 2002 April and August SHINE campaign events. Since their main characteristics have already been reported in Tylka et al. (2005, 2006) and Tylka & Lee (2006), the reader is referred to these publications for more general details.

In this work the first question we address is whether, in the solar wind frame, the field-aligned first-order anisotropy of ions is different between the April and August events. Note that in this paper the ion anisotropy is determined relative to the solar wind frame, in which the scattering centers are approximately frozen and the ions will become isotropic in the absence of other influences. This is the reference frame in which to observe small anisotropies and their reversals. If the answer to our first question is positive, our second question will be whether the difference can be attributed to the transient characteristic differences of ion-reflecting boundaries, which should be recognizable from ICME, solar flare, IMF, and solar wind observations. Finally, our third question is what other high-energy characteristics of SEPs would be affected by the difference in ion-reflecting boundaries.

Data from the *Wind*, *IMP*, and *GOES* spacecraft are used in this work. We first present the observed data on the ion first-order anisotropy, high-energy proton duration, and Fe/O ratio in both events. Then, we discuss the formation of a transient reflecting boundary and its implication on changing high-energy characteristics of SEPs.

2. OBSERVATIONS

2.1. *Observed Data*

In addition to the *Wind* and *IMP 8* spacecraft data used in our previous work (Tan et al. 2007), the high-energy proton data in the NOAA *GOES* spacecraft[6] are also used in the present work. Unlike data from *Wind* and *IMP 8*, the *GOES* sensors provide no information on ion flow directions.

Since the power-law index γ of the ion phase-space distribution function is involved in the calculation of the first-order anisotropy of ions in the solar wind frame, $\boldsymbol{A}_{1s}$, knowledge of the ion energy spectra is necessary. While the energy spectrum of heavy ions is obtained from *Wind*/LEMT data, the proton spectrum is deduced from *IMP 8* measurements. In the absence of *IMP 8* data we have developed a technique to deduce the proton spectrum from NOAA *GOES* observations.

[6] See http://spidr.ngdc.noaa.gov/spidr.

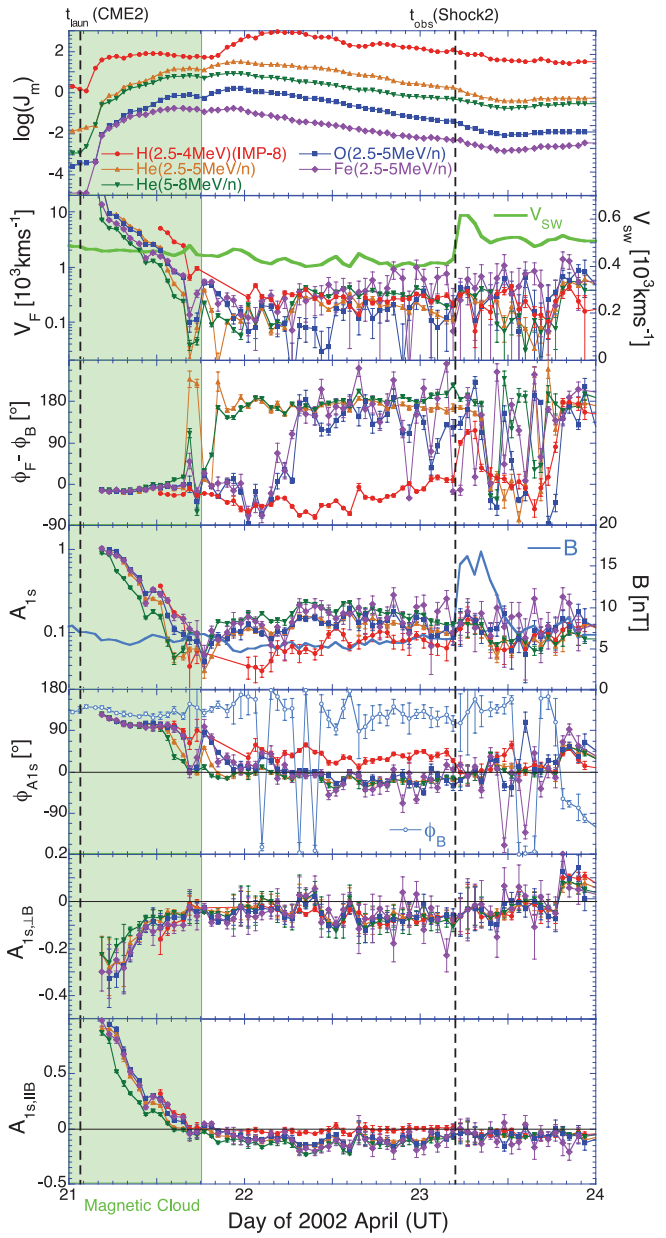

FIG. 2.—Time profiles of the ion logarithmic differential intensity ($\log(J_m)$, where J_m[cm^{-2} s^{-1} sr^{-1} (MeV nucleon^{-1})$^{-1}$]), the magnitude (V_F) of the bulk flow velocity $\boldsymbol{V}_F$ relative to the spacecraft frame, and the difference between the azimuthal angle of ϕ_F of $\boldsymbol{V}_F$ and the azimuthal angle ϕ_B of IMF ($\phi_F - \phi_B$), the magnitude (A_{1s}) and azimuthal angle (ϕ_{A1s}) of the ion first-order anisotropy in the solar wind frame ($\boldsymbol{A}_{1s}$), and the $\boldsymbol{A}_{1s}$ components perpendicular and parallel to the projected component of $\boldsymbol{B}$ on the ecliptic plane, $A_{1s,\perp B}$ and $A_{1s,\parallel B}$, for the 2002 April 21 event.

2.2. *Intensity-Time Profiles of Ions*

Intensity-time profiles of ions in the April and August events are shown in the top panels of Figures 2 and 3, respectively, where the dashed vertical lines indicate the launch time of the primary CME 2, $t_{\rm laun}$(CME 2), and the observation time of the IP shock (Shock 2) that was driven by CME 2, $t_{\rm obs}$(Shock 2). In addition, for the April event, from the near-Earth ICME table given in Cane & Richardson (2003) it is seen that a magnetic cloud (MC) appeared between April 20 00:00 (UT) and April 21 18:00 (UT), as denoted in Figure 2 by the shaded green region.

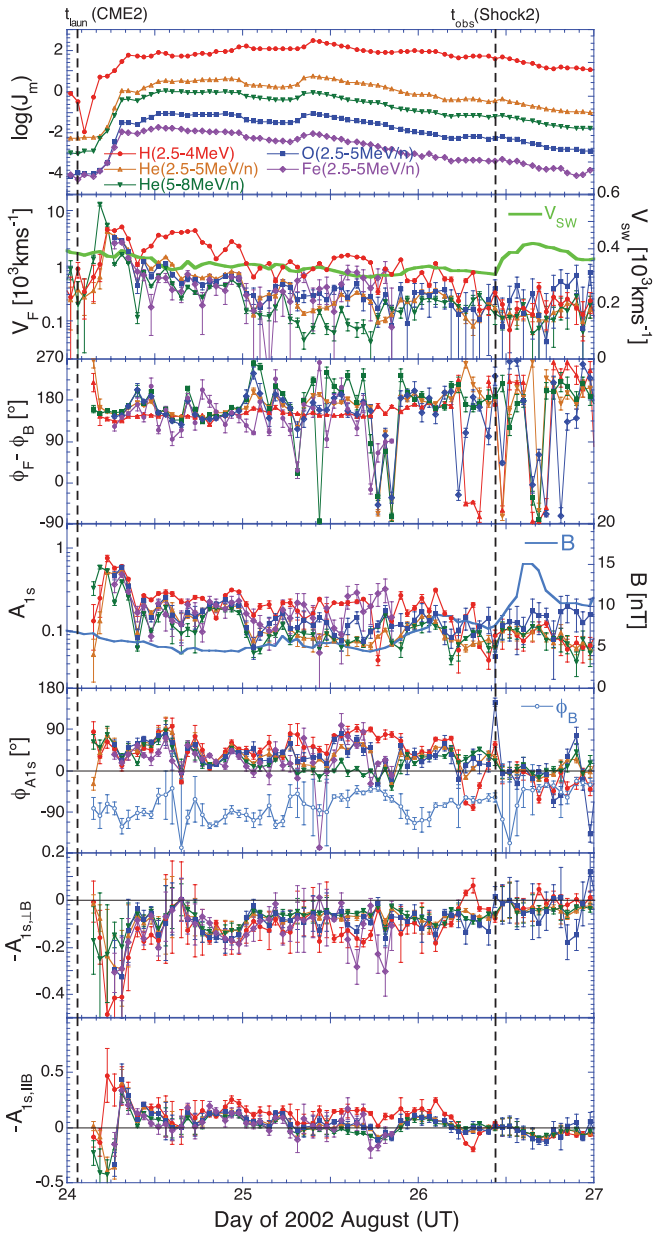

FIG. 3.—Same as Fig. 2, but for the 2002 August 24 event.

From the omnidirectional intensity data of ions, we first calculate the ion differential energy spectrum, from which the logarithmic differential intensity, $\log(J_m)$, of ions given at the mean energy T_m of selected energy channel is obtained. Upstream of IP shocks for both the April and August events, we observe $T_m \sim 3.6$ and ~ 6.1 MeV nucleon^{-1} for the *Wind*/LEMT low-energy (LE) ($T = 2.5$–5 MeV nucleon^{-1}) and high-energy (HE) ($T = 5$–8 MeV nucleon^{-1}) ion channels, respectively. For these, the lack of an intensity peak at the time of IP shock passage suggests that the effect of ion acceleration at 1 AU by local IP shocks was insignificant. In addition, in the April event additional intensity enhancements of ions were seen out of the MC region, in particular for protons.

2.3. *Bulk Flow Velocity of Ions*

The bulk flow velocity $\boldsymbol{V}_F$ of ions (Tan et al. 2007) is a measurement of ion anisotropy in the spacecraft frame. In the second and third panels of Figures 2 and 3 we plot the time profiles of its magnitude V_F and longitudinal angle ϕ_F, respectively. From the event onset, a decrease of V_F with time is generally seen for all ions. The time variation of ϕ_F, however, is significantly different between protons and heavy ions. Since the ion angular distribution measured on *Wind*/LEMT is relative to the longitudinal angle ϕ_B of the IMF, instead of ϕ_F we plot the angular difference $\phi_F - \phi_B$ in the third panel. In the April event $\boldsymbol{V}_F$ of both protons and heavy ions began along $+\boldsymbol{B}$. Then heavy ions turned their $\boldsymbol{V}_F$ to the $-\boldsymbol{B}$, while protons kept their $+\boldsymbol{B}$ direction. In contrast, in the August event both protons and heavy ions kept their $\boldsymbol{V}_F$ along the $-\boldsymbol{B}$ direction.

While the obvious difference of $\boldsymbol{V}_F$ between the two events can be attributed to the presence or absence of a nearby reflecting boundary for the SEPs in the April and August events, respectively (Tan et al. 2007), the details of $\boldsymbol{V}_F$ reversal in the April event bothers us. It is seen that O and Fe ions at given ion velocity (i.e., energy per nucleon) reversed their $\boldsymbol{V}_F$ at April 22 $\sim$06:00 (UT), which should be relevant to the flow reversal of heavy ions as observed in Tan et al. (2007). In contrast, both He ions at the same and higher velocity showed a magnitude minimum and directional reversal of $\boldsymbol{V}_F$ at $\sim$1/2 day earlier (April 21 $\sim$18:00 UT), indicating the possible effect of magnetic discontinuity on $\boldsymbol{V}_F$ occurring at the MC boundary. In fact, during the 1998 May 2 MC event, at the MC boundary a nearly zero field-aligned component of ion first-order anisotropies was also seen by Torsti et al. (2004) for 17–22 MeV protons (see their Fig. 1), and by us for a few MeV per nucleon ions (data not shown here). To avoid complications near the MC boundary, in our further examination of the April event we will concentrate on later times when the *Wind* spacecraft was out of the MC.

2.4. *First-Order Anisotropy of Ions in the Solar Wind Frame*

It is interesting to note that, as one kind of ICMEs, the MC should also be driven by the solar wind. Similarly, the effect of magnetic discontinuity at the MC boundary should be clearly seen in the solar wind frame. That raises another reason to examine the ion first-order anisotropy in the solar frame. Based on the bulk flow velocity $\boldsymbol{V}_F$ measured in the spacecraft frame, we have developed a technique to deduce the ion first-order anisotropy $\boldsymbol{A}_{1s}$ in the solar wind frame. According to equation (4) of Tan et al. (2007), we have

$$\boldsymbol{A}_{1s} = \gamma(\boldsymbol{V}_F - \boldsymbol{V}_{\rm sw})/v, \qquad (1)$$

where v is the ion speed, γ is the power-law index of the ion phase-space distribution function, and $\boldsymbol{V}_{\rm sw}$ is the solar wind velocity. From equation (1) it is seen that at $V_F \gg V_{\rm sw}$, $\boldsymbol{A}_{1s} \approx \gamma\,\boldsymbol{V}_F/v$, while at $V_F \ll V_{\rm sw}$, $\boldsymbol{A}_{1s}$ is antisunward.

For the April and August events, the magnitude A_{1s} and azimuthal angle ϕ_{1s} of $\boldsymbol{A}_{1s}$ are shown on the fourth and fifth panels of Figures 2 and 3, respectively. In both events during the "onset" phase we have $V_F > V_{\rm sw}$, and during the "plateau" phase we have $V_F < V_{\rm sw}$, where the classification of event phases is according to Lee (2005). Consequently, during the onset phase $\boldsymbol{A}_{1s}$ showed a forward streaming along $\boldsymbol{B}$, while during the plateau phase $\boldsymbol{A}_{1s}$ was along $-\boldsymbol{V}_{\rm sw}$, toward the Sun.

Since in the August event (see Fig. 3), the onset of MeV nucleon^{-1} ions appeared significantly later than the launch time of the primary CME 2 [i.e., $t_{\rm laun}$(CME 2)]; during the first few hours in the event we indeed detected the background particle stream left by previous SEP events. In addition, since in the August event the polarity of $\boldsymbol{B}$ was mainly sunward (see fifth panel of Fig. 3), the Y-axis on the bottom panel of Figure 3 is chosen to

be $-A_{1s,\|B}$. As a result, the positive *Y*-axis on the bottom panels of Figures 2 and 3 always points antisunward. Thus during the onset phase in both events all ions showed outward streaming. The situation, however, was different during the plateau phase of corresponding ions. In the April event while protons had no field-aligned stream ($A_{1s,\|B} \sim 0$), all heavy ions showed sunward streaming. A nearly zero stream of ions was reached at the boundary of MC, which was shown in Figures 2, 4, and 5 as the shaded green region. In contrast, in the August event both protons and heavy ions kept their forward streaming away from the Sun.

The two-dimensional $\boldsymbol{A}_{1s}$ vector measured by the *Wind*/LEMT sensor can be decomposed into two components, $A_{1s,\|B}$ and $A_{1s,\perp B}$, parallel and perpendicular to the projected component of $\boldsymbol{B}$ on the ecliptic plane, respectively. Since during the upstream period between $t_{\rm laun}$ (CME 2) and $t_{\rm obs}$ (Shock 2) in the April and August events the magnetic field $\boldsymbol{B}$ was nearly in on the ecliptic plane (in the GSE system the mean latitudinal angle of $\boldsymbol{B}$ was $10^\circ \pm 20^\circ$ and $-18^\circ \pm 14^\circ$, respectively), these components can approximately represent the projected components of the first-order anisotropy vector along the directions parallel and perpendicular to $\boldsymbol{B}$, respectively. Note that the positive direction of $A_{1s,\|B}$ is given along $\boldsymbol{B}$, and the positive direction of $A_{1s,\perp B}$ shows a $+90^\circ$ (anticlockwise) angle to that of $A_{1s,\|B}$. The time profiles of $A_{1s,\perp B}$ and $A_{1s,\|B}$ for the April and August events are shown on the sixth and bottom panels of Figures 2 and 3, respectively. It can be seen that both events had similar $A_{1s,\perp B}$ profiles, which could be caused by north-south density gradients and/or perpendicular diffusion (Zhang et al. 2003). These effects are generally difficult to estimate, because of the unknown diffusion tensor and particle density gradient. Since we are concerned mainly with the ion anisotropy originating from ion streaming, the emphasis of our examination is put on $A_{1s,\|B}$, the field-aligned component of $\boldsymbol{A}_{1s}$.

From the bottom panel of Figure 2, it can be seen that inside the MC the field-aligned antisunward anisotropy $A_{1s,\|B}$ of all ions decreased with time. As in the 1998 May 2 MC event (Torsti et al. 2004), we observe a nearly zero $A_{1s,\|B}$ at the MC boundary. Furthermore, out of the MC the $A_{1s,\|B}$ of all heavy ions changed to be sunward, while protons kept a nearly zero $A_{1s,\|B}$. Therefore, by comparing Figure 2 with Figure 3 we see that in the solar wind frame, during the plateau phase of corresponding ions the main difference between the April and August events in particle streaming is that a streaming reversal of heavy ions was observed in the April event, but not in the August event. In § 3 we will consider other characteristic variation of $A_{1s,\|B}$ during different phases.

2.5. *IMF and Solar Wind Observations*

Similar to the analysis of the 2001 September 24 event shown in § 1.4, here we examine whether the IMF and solar wind data are favorable to the presence and absence of a nearby reflecting boundary of SEPs in the 2002 April 21 and August 24 events, respectively. In the top panels of Figure 4 we plot the time profiles of B and $V_{\rm sw}$ in the April event as measured by the *Wind* spacecraft during ~1 week prior to the launch of the primary CME 2 [i.e., $t_{\rm laun}$(CME 2)]. Before $t_{\rm laun}$(CME 2) there were at least two IP shocks observed at $t_{\rm obs}$(Shock 1-1) and $t_{\rm obs}$(Shock 1-2). The CME corresponding to the first shock, whose observation time was at April 17 11:02 (UT), should have less effect on the April event because of its distant location. We hence only consider the CME 1-2, which was relevant to the Shock 1-2.

Similar to what we did for the 2001 September 24 event, here we assume that the average speed of the preceding CME 1-2 between the Sun and 1 AU was between $V_{\rm sw1}$(~600 km s^{-1}) and $3V_{\rm sw1}$. Thus, the launch times of CME 1-2 should be between April 16 11:00 (UT) and April 18 09:00 (UT). During the suggested time interval there was an obvious candidate event for CME 1-2, with onset time at April 17 07:50 (UT) (linear fitting). The candidate CME was a fast (1240 km s^{-1}) halo event associated with both a M2.6 X-ray flare at S14°, W34°, near the central meridian, and a gradual SEP event. In addition, from the difference between $t_{\rm laun}$(CME 1-2) and $t_{\rm obs}$(Shock 1-2), the estimated average speed of CME 1-2 between the Sun and 1 AU was 856 km s^{-1}, very close to that of the 2001 September 24 event.

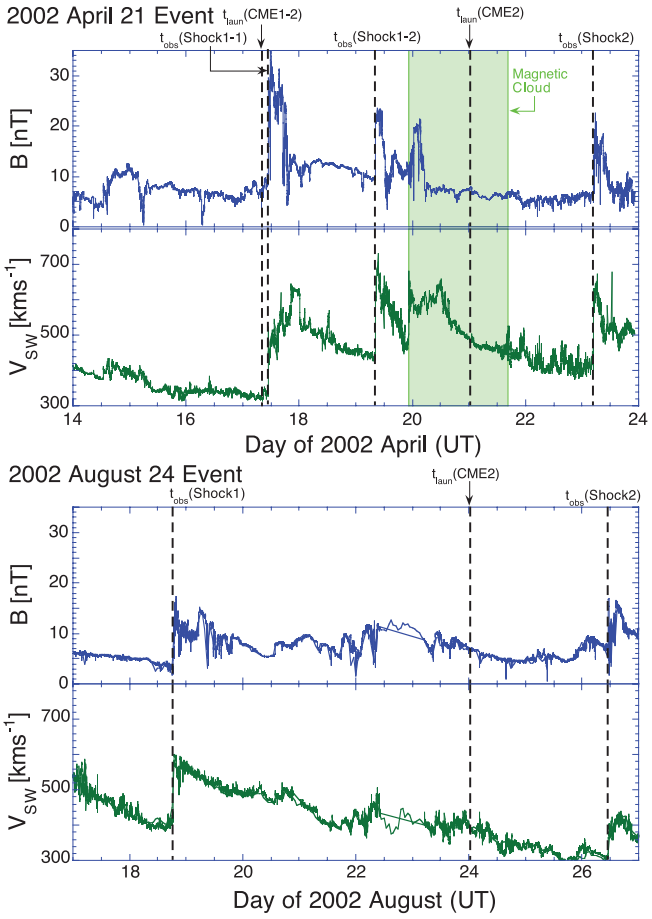

FIG. 4.—Time profiles of B and $V_{\rm sw}$ for the 2002 April 21 event (*top*) and August 24 event (*bottom*).

As shown in the top panels of Figure 4, the onset of the primary CME 2 occurred inside the MC. Therefore, during the onset phase the field lines passing the *Wind* spacecraft were probably or mostly closed. Upon exiting from the MC, however, the field lines were open completely. Because of the complexity caused by MC boundary crossing, for the 2002 April 24 event it is difficult to draw a cartoon of field line configuration (as we did in Fig. 1 for the 2001 September 24 event). Nevertheless, the only real questions are whether there were any reasonable observed driver CMEs to associate with the interplanetary shocks. The CME details are not relevant here. We hence expect that between the preceding CME and the IP shock prior to it there would exist a magnetic mirror that played the role of the outer reflecting boundary of SEPs.

Finally, we briefly mention IMF and solar wind observations in the August event, whose B and $V_{\rm sw}$ data are shown on the bottom panels of Figure 4, where the gap in *Wind* data has been filled

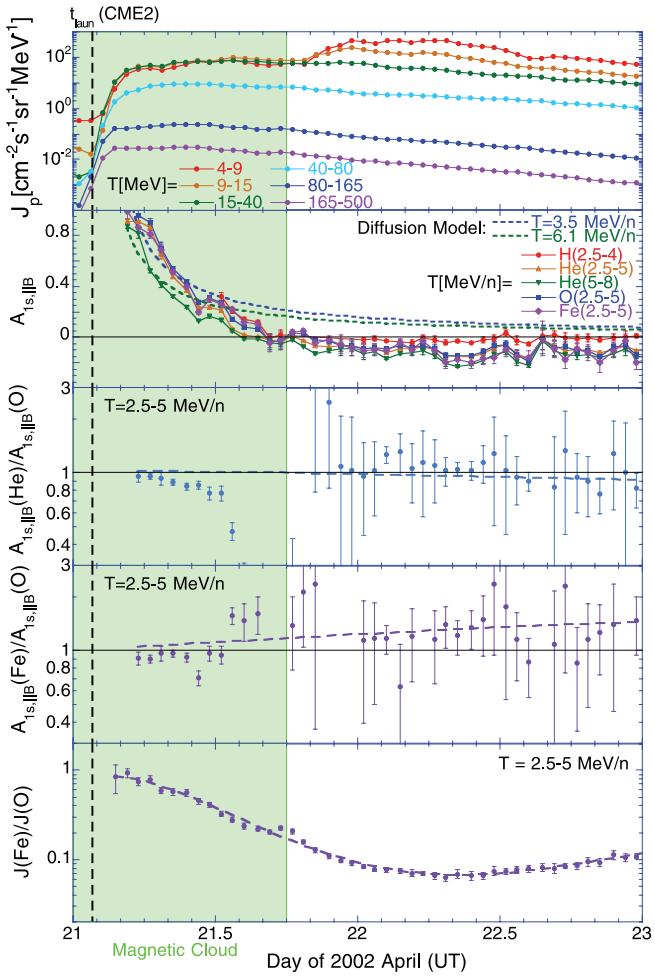

FIG. 5.—Time profiles of high-energy protons from *GOES-8* observations, the field-aligned anisotropy $A_{1s,B}$ as compared with the prediction of the diffusion model, the $A_{1s,\|B}$(He)/$A_{1s,\|B}$(O), $A_{1s,\|B}$(Fe)/$A_{1s,\|B}$(O), and J(Fe)/J(O) ratios for the 2002 April 21 event.

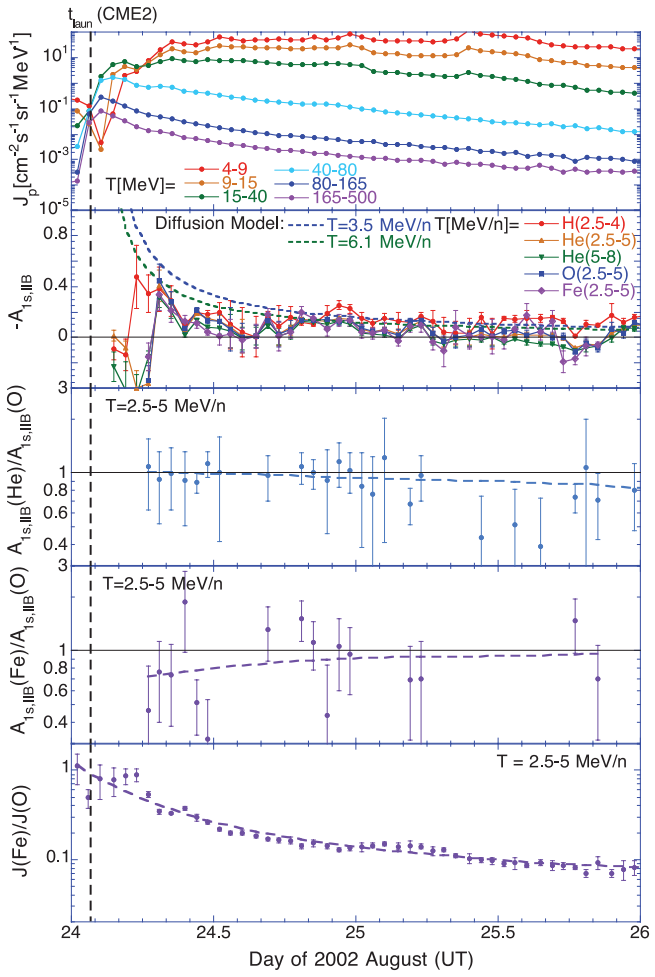

FIG. 6.—Same as Fig. 5, but for the 2002 August 24 event.

with the OMNI combined data.[7] There was no peak $B_m \geq 15$ nT until ~5 days prior to t_{laun}(CME 2), indicating the absence of a nearby reflecting boundary in the August event. Nevertheless, a distant reflecting boundary for SEPs may still exist, as evidenced from the observation of the IP shock (Shock 1) prior to the primary CME (CME 2), as shown on the bottom panel of Figure 4.

3. DISCUSSIONS

3.1. *Duration of High-Energy Proton Intensities*

Intensity-time profiles of high-energy protons measured by the *GOES-8* spacecraft are shown on the top panels of Figures 5 and 6 for the April and August events, respectively. From the panels we note the following facts. (1) The time to reach the intensity maximum in the August event was shorter than that in the April event. (2) After passing the maximum, the proton intensity in the August event showed a relatively fast decay, with the decay rate being both time and proton energy dependent. In contrast, the proton intensity in the April event showed a relatively slow decay with an exponential decay rate independent of proton energies, which is consistent with the calculations of Reames et al. (1996) and Ng et al. (2003) behind IP shocks and the simulation of Kocharov et al. (2005) in looplike MCs. (3) In the April event an intensity enhancement of <15 MeV protons was seen outside the MC region, while >15 MeV protons showed a continuous exponential decay with time when the MC boundary was crossed. (4) Similar to Tylka et al. (2005), we observe that the duration of high-energy proton intensities in the August event was much shorter than in the April event. Therefore, the observed difference in high-energy proton durations between the two events is in support of our speculation discussed in § 1.5.

3.2. *Characteristic Variations of Field-Aligned First-Order Anisotropy of Ions in the Solar Wind Frame*

In the region upstream of IP shocks, the $A_{1s,\|B}$ data in the April and August events are plotted on the second panels of Figures 5 and 6, respectively. From Figure 5 it is seen that in the April event during the onset phase $A_{1s,\|B}$ was approximately ion velocity-dependent, because of the near overlap of $A_{1s,\|B}$ plots for various ion species given at same ion velocity. Since the diffusion model (Parker 1963) predicts an ion-velocity-dependent field-aligned anisotropy, we compare the model prediction with observations. In the radial (r) diffusion model with the mean free path $\lambda = \lambda_0 r^{\beta}$, where λ_0 and β are constant, for an impulsive release of ions at time $t = 0$ and $r = 0$, the predicted field-aligned first-order anisotropy is (see Appendix C of Ng et al. 2003)

$$A_{1s,B} = 3r/[(2-\beta)vt]. \quad (2)$$

[7] See http://cdaweb.gsfc.nasa.gov.

Taking into account the Archimedean spiral structure of IMF, we substitute $r = 1.15$ AU into equation (2) in order to calculate the time profiles of $A_{1s,B}$ given at the mean energies $T_m \sim 3.6$ and $\sim$6.1 MeV nucleon^{-1} for the *Wind*/LEMT LE and HE ion channels, respectively. Here $\beta = 0.4 \pm 0.1$ is estimated from the comparison of high-energy proton intensities predicted by the diffusion model with *GOES-8* observations in the August event (also see Ng & Reames 1994). The $A_{1s,\|B}$ values predicted by the diffusion model are shown in the second panels of Figures 5–6 as the dotted lines.

In view of the fact that no free parameter is introduced into equation (2), during the onset phase in the April event the consistency between the prediction and observation should be acceptable. During the plateau phase, however, the prediction and observation are opposite in phase, indicating a streaming reversal of heavy ions in the solar wind frame. In addition, for protons we see that $A_{1s,\|B} \sim 0$, implying a balance between the forward stream of protons freshly accelerated by the IP shock and the backward stream of reflected protons earlier accelerated near the Sun; or perhaps it only implies a uniform radial intensity distribution of protons throughout the flux tube.

Moreover, during the plateau phase in the April event we observed that the $A_{1s,B}$ value was different among different ion species given at same ion velocity. We are interested in exploring the nature of such difference. Thus, we plot the $A_{1s,\|B}(\mathrm{He})/A_{1s,\|B}(\mathrm{O})$ and $A_{1s,\|B}(\mathrm{Fe})/A_{1s,\|B}(\mathrm{O})$ ratios on the third and fourth panels of Figure 5, respectively. Note the scarcity and scattering of data points during April 21 14:00–22:00 (UT), when the MC boundary was crossed. In order to find the mean value of the above ratios during the plateau phase, we calculate their weighted average over the period of 2002 April 22–23 (UT). We find $A_{1s,\|B}(\mathrm{He})/A_{1s,\|B}(\mathrm{O}) = 1.01 \pm 0.04$ and $A_{1s,\|B}(\mathrm{Fe})/A_{1s,\|B}(\mathrm{O}) = 1.2 \pm 0.1$. Since He and O ions with nearly same rigidities had same $A_{1s,\|B}$ value, and the $A_{1s,\|B}$ value of higher rigidity Fe ions was greater than that of lower rigidity O ions, we conclude that in the April event during the plateau phase $A_{1s,\|B}$ was ion-rigidity-dependent.

The situation is different in the August event. Because of the delayed launch of MeV nucleon^{-1} ions, we cannot examine its onset phase in detail. During the plateau phase, however, the prediction of the diffusion model was consistent with the observation, in either polarity or magnitude of $A_{1s,\|B}$. The $A_{1s,\|B}(\mathrm{He})/A_{1s,\|B}(\mathrm{O})$ and $A_{1s,\|B}(\mathrm{Fe})/A_{1s,\|B}(\mathrm{O})$ ratios are also shown in the third and fourth panels of Figure 6, respectively, although no firm conclusion can be extracted because of the poor quality of data, resulting from the extremely small values of $A_{1s,\|B}$.

3.3. *Time Profiles of* Fe/O *Ratios*

We calculate the Fe/O ratio over different ion velocity (energy per nucleon) ranges. We first parameterize the energy spectrum of ions by using polynomial fitting, from which the ion intensity integrated over a given velocity window is deduced by numerical integration. From the integrated ion intensities we then calculate the Fe/O ratio. Our deduced Fe/O ratio at $T = 2.5$–5 MeV nucleon^{-1} is shown in the bottom panels of Figures 5 and 6 for the April and August events, respectively.

In both events, starting from the event onset, the Fe/O ratio presents an exponential decline with time, although the detail of time variations is different. The Fe/O ratio in the April event had a minimum (Fig. 5), as predicted by Ng et al. (2003), while the ratio shows a monotonic decrease in the August event (Fig. 6). Why would the Fe/O ratio enhance again after passing its minimum in the April event? We believe that the enhancement of the Fe/O ratio could be relevant to the observed $A_{1s,\|B}(\mathrm{Fe})/A_{1s,\|B}(\mathrm{O}) > 1$, which implies that along the magnetic field direction Fe ions have a greater sunward flow than O ions. Consequently, more Fe ions should appear in the backward stream, leading to an increase of Fe/O ratios during the plateau phase. Effectively, the sunward-flowing ions reflected from the mirror retain the high Fe/O values seen early in the event.

3.4. *Comparison with Previous SHINE Event Analysis*

In this work we add the anisotropy data of ions to the analysis of two SHINE campaign events previously reported in Tylka et al. (2005, 2006) and Tylka & Lee (2006). We are mainly concerned with the change of ion transport in the 2002 April 21 event due to the apparent presence of a nearby reflecting boundary of SEPs. Through our analysis we have observed the streaming reversal of heavy ions in the solar wind frame, indicating the possible existence of a transient reflecting boundary of SEPs. Evidence gathered from heliospheric, IMF, and solar wind observations indicates that the magnetic mirror located between the preceding CME and the IP shock prior to it forms the boundary. In the April event, during the onset phase the field-aligned first-order anisotropy of ions in the solar wind frame is ion-velocity-dependent, while during the plateau phase the reversed streaming of ions is ion-rigidity-dependent.

It should be admitted that the presence of a nearby reflecting boundary for SEPs would significantly affect the characteristics of SEPs in the April event. For example, the reservoir effect caused by the boundary would increase the peak intensity and duration of high-energy particles, leading to a high particle fluence integrated over the entire SEP event in space. In addition, since any boundary would have finite cutoff rigidity, at sufficiently high velocity (energy per nucleon), Fe ions may freely escape from the boundary, while lower rigidity O ions would still be reflected. As a result, the boundary could cause a decrease of Fe/O ratios at very high energies. However, this latter effect should be indistinguishable from similar spectral "knees" produced by rigidity-dependent trapping during acceleration.

In the previous SHINE event analysis, the variation of event durations, spectral shapes, and Fe/O ratios were attributed to the interplay between shock geometry and seed population (Tylka et al. 2005, 2006; Tylka & Lee 2006). Particle reflection at a boundary beyond 1 AU is unlikely to influence shock acceleration close to the Sun and will not affect the magnitude of the Fe/O ratio, but will affect SEP event duration, as well as the time and energy variation of Fe/O. Our work does not question the importance of seed populations and shock geometry in determining the Fe/O ratio. However, the new observation presented in this work suggests that boundary reflection is important to the interpretation of SEP characteristics observed during the April event.

4. SUMMARY

We have made comparative studies of the 2002 April and August SEP events, which had very similar solar progenitors but showed distinctly different high-energy characteristics of SEPs. Our main findings are as follows.

1. In the August event, the field-aligned anisotropy in the solar wind frame showed no signal of reversal, while in the April event a streaming reversal of all heavy ions were observed during the plateau phase.

2. In the April event, the field-aligned anisotropy of both protons and heavy ions in the solar wind frame was nearly zero at the boundary of the magnetic cloud.

3. In the April event, a shock wave from a preceding CME with a peak magnetic field strength of $\sim$20 nT was observed

within ~1.5 day before the launch of the primary CME. In the August event, however, there was no preceding CME within ~5 days before the primary CME.

4. In the April event the peak intensity and duration of high-energy protons were much greater than that in the August event. In addition, in the August event the decay time of high-energy protons was relatively short and proton-energy-dependent. In contrast, in the April event the long decay time of high-energy proton intensities was independent of proton energies.

5. In the April event the minimum of Fe/O ratios was consistent with a higher backward field-aligned anisotropy for Fe ions than for O ions during the plateau phase.

We have been able to interpret these observations in terms of the presence of a nearby transient reflecting boundary that modified the properties of the 2002 April 21 SEP event, and the absence of such a boundary in the 2002 August 24 SEP event. Particle reflection at a boundary beyond 1 AU is unlikely to influence shock acceleration close to the Sun and will not affect the magnitude of the Fe/O ratio, but will affect SEP event duration as well as the time and energy variation of Fe/O. Our work does not question the importance of seed populations and shock geometry in determining the Fe/O ratio. However, the new observation presented in this work suggests that boundary reflection is important to the interpretation of SEP characteristics observed during the April event.

We appreciate the use of data provided by the NSSDC CDAWeb, NOAA, and the *SOHO* LASCO CME catalog, which is generated and maintained at the CDAW Data Center by NASA and the Catholic University of America in cooperation with the Naval Research Laboratory. We thank K. Ogilvie, A. Tylka, and X. Shao for many helpful discussions. We also thank the anonymous reviewer for his/her valuable comments. C. K. N. is supported under NASA grants LWS04-0000-0076 and SHP04-0016-0024.

REFERENCES

Bieber, J. W., et al. 2002, ApJ, 567, 622
Cane, H. V., Reames, D. V., & von Rosenvinge, T. T. 1988, J. Geophys. Res., 93, 9555
Cane, H. V., & Richardson, I. G. 2003, J. Geopys. Res., 108, A41156
Desai, M. I., et al. 2003, ApJ, 588, 1149
———. 2004, ApJ, 611, 1156
Forman, M. A. 1970, Planet. Space Sci., 18, 25
Gloeckler, G., et al. 1984, Geophys. Rev. Lett., 11, 603
Kocharov, L., et al. 2005, J. Geophys. Res., 110, A12S03
Lee, M. A. 1983, J. Geophys. Res., 88, 6109
———. 2005, ApJS, 158, 38
Ng, C. K., & Reames, D. V. 1994, ApJ, 424, 1032
Ng, C. K., Reames, D. V., & Tylka, A. J. 2003, ApJ, 591, 461
Parker, E. N. 1963, Interplanetary Dynamical Processes (New York: Interscience)
Reames, D. V. 1999, Space Sci. Rev., 90, 413
Reames, D. V., Barbier, L. M., & Ng, C. K. 1996, ApJ, 466, 473
Reames, D. V., & Ng, C. K. 2002, ApJ, 577, L59
Reames, D. V., Ng, C. K., & Berdichevsky, D. 2001, ApJ, 550, 1064
Roelof, E. C., et al. 1992, Geophys. Res. Lett., 19, 1243
Sarris, E. T., & Malandraki, O. E. 2003, Geophys. Res. Lett., 30(21), 2079
Tan, L. C., Reames, D. Y., & Ng, C. K. 2007, ApJ, 661, 1297
Tan, L. C., et al. 1992a, J. Geophys. Res., 97, 1597
———. 1992b, J. Geophys. Res., 97, 179
Torsti, J. Rihonen, E., & Kocharov, L. 2004, ApJ, 600, L83
Tylka, A. J., & Lee, M. A. 2006, ApJ, 646, 1319
Tylka, A. J., et al. 2005, ApJ, 625, 474
———. 2006, ApJS, 164, 536
von Rosenvinge, T. T., et al. 1995, Space Sci. Rev., 71, 155
Zhang, M., Jokipii, J. R., & NcKibben, R. B. 2003, ApJ, 595, 493